

Fuzzy hybrid control of a wind-excited tall building

Joowon Kang¹ and Hyun-Su Kim*²

¹School of Architecture, Yeungnam University, Gyeongsan-si, Gyeongbuk 712-749, Korea

²Division of Architecture, Sunmoon University, Asan-si, Chungnam 336-708, Korea

(Received September 9, 2009, Accepted July 10, 2010)

Abstract. A fuzzy hybrid control technique using a semi-active tuned mass damper (STMD) has been proposed in this study for mitigation of wind induced motion of a tall building. For numerical simulation, a third generation benchmark is employed for a wind-excited 76-story building. A magnetorheological (MR) damper is used to compose an STMD. The proposed control technique employs a hierarchical structure consisting of two lower-level semi-active controllers (sub-controllers) and a higher-level fuzzy hybrid controller. Skyhook and groundhook control algorithms are used as sub-controllers. When a wind load is applied to the benchmark building, each sub-controller provides different control commands for the STMD. These control commands are appropriately combined by the fuzzy hybrid controller during real-time control. Results from numerical simulations demonstrate that the proposed fuzzy hybrid control technique can effectively reduce the STMD motion as well as building responses compared to the conventional hybrid controller. In addition, it is shown that the control performance of the STMD is superior to that of the sample TMD and comparable to an active TMD, but with a significant reduction in power consumption.

Keywords: fuzzy logic controller; hybrid control; semi-active tuned mass damper; skyhook; groundhook; wind-excited tall building.

1. Introduction

The use of a conventional tuned mass damper (TMD) is undoubtedly a simple, inexpensive and reliable means to suppress the undesired vibrations of structures. However, its performance is limited because of fixed damper parameters. The very narrow band of suppression frequency, the ineffective reduction of non-stationary vibration, and the sensitivity problem due to off-tuning are the inherent limitations of the passive TMD (Den Hartog 1956, Warburton and Ayorinde 1980). The effectiveness of the TMD can be significantly enhanced by the introduction of an active force to act between the structure and the TMD, i.e., the active TMD (ATMD) (Chang and Soong 1980, Ankireddi and Yang 1996). Although the ATMD can demonstrate a superior performance over the optimal passive TMD, the active system is more costly, more complex, and needs routine maintenance, all of which renders it less reliable than the passive system. Recognizing the performance benefits as well as the lack of stability of active systems, the concept of a semi-active tuned mass damper (STMD) has been introduced. Recently, various studies on the STMD have been

*Corresponding author, Professor, E-mail: hskim72@sunmoon.ac.kr

conducted for the vibration control of civil structures. Hrovat *et al.* (1983) investigated the benefits of using an STMD for the suppression of wind-induced vibration. Assuming a specific type of wind loading, they reported a similar performance between the STMD and ATMD. Hidaka *et al.* (1999) conducted an experimental study of an STMD system coupled with a three-story building model under support ground motion. Pinkaew and Fujino (2001) studied the control effectiveness of an STMD with variable damping under harmonic excitation. Nagarajaiah and Varadarajan (2000) developed an STMD using a variable stiffness device and they have shown its effectiveness analytically and experimentally by using a small-scale three story structural model. Koo *et al.* (2006) presented an experimental robustness analysis of a semi-active tuned vibration absorber (TVA) subject to structural mass off-tuning using a magnetorheological (MR) damper.

Most previous research has focused on the control performance evaluation of an STMD by using a simplified single or several DOFs structures and idealized external loads, such as harmonic or random dynamic forces. In order to conduct a more practical research, this study uses a full-scale 76-story benchmark building subjected to a wind excitation (Yang *et al.* 2004). Across wind load data obtained from wind tunnel tests are used as an excitation in the numerical simulation.

There are many control strategies for semi-active damping control in the literature (Ricciardella *et al.* 2000, Liu *et al.* 2005, Jansen and Dyke 1999). Among them, the “skyhook” and “groundhook” control policies are favorably used because of their simplicity and effectiveness. They have also shown good control performances for the vibration control of civil structures as well as vehicle applications (Liu *et al.* 2005, Koo *et al.* 2006, Narasimhan *et al.* 2006). Koo *et al.* (2004) evaluated four different types of groundhook control algorithms for semi-active TVA and reported that the displacement based on-off groundhook controller showed the best performance among the considered control policies. In their study, the control performances were evaluated using peak transmissibility criteria. However, in addition to the control performance, a constraint on the maximum allowable displacement of the STMD is important for practical application and it must be considered in the design of the STMD. To limit the stroke of the STMD, an overdamping or additional damper may therefore be necessary, which results in a lower efficiency of the STMD, and thus in a larger response of the building structure.

To overcome this problem, a fuzzy hybrid control technique has been proposed in this study to reduce the STMD motion without an accompanying increase in dynamic responses of the building structure. The purpose of this study is to achieve the required control effect of the benchmark problem and to satisfy the control device capacity constraints. In this study, the STMD consisting of an MR damper is employed to control the benchmark building. The proposed control algorithm uses a two step control procedure that consists of a fuzzy hybrid controller at the higher level and two sub-controllers (skyhook and groundhook controllers) at the lower level. It is known that a skyhook controller effectively reduces an STMD motion and that a groundhook controller shows good control performance for the suppression of building responses (Koo *et al.* 2004, Narasimhan and Nagarajaiah 2006, Karnopp *et al.* 1974, Setareh 2001). The fuzzy hybrid controller calculates the participation of each sub-controller in real time by appropriately combining the control commands generated by two sub-controllers using a weighted sum approach. When carrying this out, a suitable weighting factor is promptly determined based on the dynamic responses of the STMD and building structure. The control performance of the proposed fuzzy hybrid controller is compared to that of a conventional hybrid controller using a fixed weighting factor. The effectiveness of the STMD controlled by the proposed controller is evaluated by comparing it with that of the sample TMD, and the ATMD proposed in the benchmark problem (Yang *et al.* 2004). The sample TMD has an

inertial mass of 500 tons and its damping ratio is 20%. This sample TMD is tuned to the first modal frequency of the benchmark building.

2. Configuration of semi-active tuned mass damper

Many of previous studies used an idealized variable damping device to compose an STMD for numerical simulation. The minimum damping coefficient of an idealized variable damping device is usually set to zero and the maximum damping coefficient is assumed to be unlimited. In general, the damping coefficient of an idealized variable damping device is directly controlled in numerical simulation. However, in practical application, the electrical signal rather than the damping coefficient is usually regulated by the control algorithm. Therefore, for a more practical study, an MR damper is employed to compose an STMD system instead of an idealized variable damping device as shown in Fig. 1. An MR damper is known to be one of the typical smart devices using MR fluid, which have damping characteristics that can be varied by controlling the magnetic field. The fluid yield stress and viscosity are directly dependent on the applied magnetic field strength that is controlled by the command voltage sent to the MR damper. The MR damper produces frictional damping force that is related to the fluid yield stress. Accordingly, frictional damping force of the MR damper can be controlled by changing the fluid yield stress and it can be done by controlling the command voltage sent to the MR damper. In this study, the Bouc-Wen model (Sues *et al.* 1988) is used to describe how the viscous damping force and frictional damping force (associated with the fluid yield stress) are related to the velocity and applied command voltage because this model is simple to implement and predicts well the behavior of the MR damper. From previous experimental researches on MR dampers, it is known that there is nonzero initial damping force with no applied magnetic field (i.e., at 0 V). This nonzero initial damping force is due in part to the fluid which by design has a small yield strength at zero magnetic field for stability against gravitational settling, and in part due to friction in the piston rod seal. This nonzero initial damping force is uncontrollable and it can be represented by the Bouc-Wen model as shown in Fig. 2 (passive-off case). As observed in this figure, the maximum damping force of the MR damper used in this study is approximately 100 kN. This passive-on damping force was determined by an iterative method for optimal vibration control of the 76-story benchmark building. In the iterative method, the passive-on damping force of the MR damper was evaluated from 10 kN to 300 kN with the step of 10 kN. The damping force of the MR damper is controlled by the command voltage. When the maximum

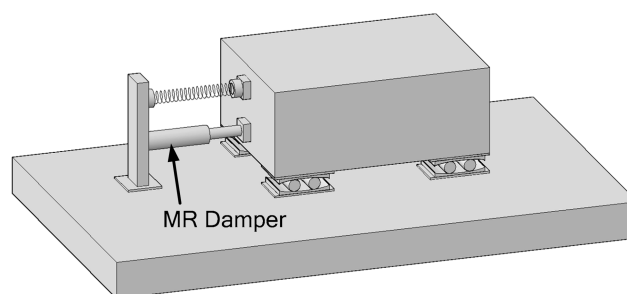


Fig. 1 Semi-active TMD system using an MR damper

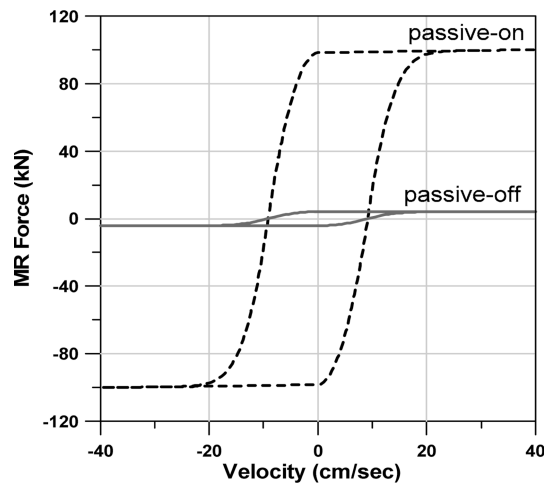


Fig. 2 Force-velocity hysteresis loop of the MR damper

damping force is required (passive-on), 5 V is sent to the MR damper, and the minimum command voltage (passive-off) is 0 V. Since an MR damper can play the role of a passive damper in the event of a power loss (i.e., 0 V), the proposed STMD will act as a passive TMD. Accordingly, the STMD in the event of a power loss will be just as stable as the passive TMD.

For a comparative study, the inertial mass of the STMD used in this study is identical to that of the sample TMD and ATMD presented in the benchmark problem, i.e., 500 tons. This is about 45% of the top floor mass, which is 0.327% of the total mass of the building. The single STMD is installed on the top floor of the 76-story benchmark building. The undamped natural frequency of the STMD is 0.16 Hz, which is the first mode natural frequency of the example building.

3. Benchmark problem

3.1 76-story benchmark building and wind excitations

The benchmark building used in this study is a 76-story 306-meter concrete office tower proposed for the city of Melbourne, Australia (Yang *et al.* 2004). The building has a square cross section with chamfers at two corners as shown in Fig. 3. This is a reinforced concrete building consisting of a concrete core and concrete frame. The core was designed to resist the majority of wind loads whereas the frame was designed to primarily carry the gravitational loads and part of the wind loads. The building is slender with a height to width ratio of 7.3. Therefore, it is wind sensitive. The total mass of the building, including heavy machinery in the plant rooms, is 153,000 metric tons. The building has been modeled by a series of vertical beam elements between adjacent floors. The rotational degrees of freedom have been removed by the static condensation, leaving only the translational degrees of freedom active. Since the coupled lateral-torsional motion is neglected in the benchmark problem and across-wind and along-wind loads are uncorrelated, building response quantities due to across-winds and along-winds can be computed independently. Based on wind tunnel data, building response quantities due to across-wind loads are much higher than that due to

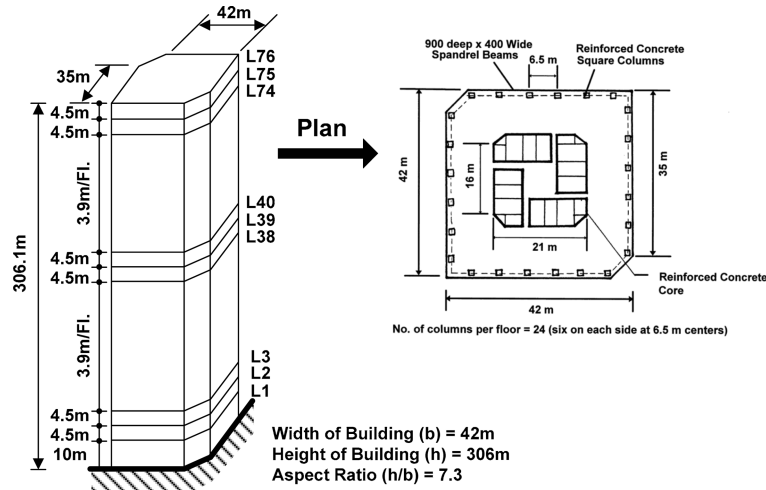


Fig. 3 76-story Benchmark building (Yang *et al.* 2004)

along-wind loads. Consequently, only the design of controller using across-wind loading is considered in the benchmark problem. Therefore, a two-dimensional analytical model is used and the rotations of the floors about the vertical axis are not considered in the numerical simulation. The resulting system of equations involving mass, stiffness, and damping matrices of the structure is solved by the Newmark-Beta integration scheme using a linear acceleration method (Ohtori *et al.* 2004). The first five natural frequencies of the structure are 0.16, 0.765, 1.992, 3.790 and 6.395 Hz, respectively. Damping ratios for the first five modes are assumed to be 1% of critical for the proportional damping matrix. The benchmark building is a long period structure having the first natural period of 6.25 sec. Since the motion of a long period structure is generally governed by the first modal response, the frequencies of the TMD, ATMD and STMD have been tuned to the first modal frequency of the structure. The sample ATMD proposed in the benchmark problem has the same mass and location as the TMD. A control algorithm for the sample ATMD was designed based on the linear quadratic Gaussian (LQG) theory. Wind forces acting on the benchmark building were obtained by wind tunnel tests. A rigid model of the 76-story benchmark building was constructed and tested in the boundary layer wind tunnel facility at the Department of Civil Engineering at the University of Sydney, Australia (Samali *et al.* 2004). For the performance evaluation of control systems, only the first 15 minutes (900 seconds) of across-wind data are used. Based on the design code for office buildings in Australia, the maximum allowable floor acceleration is 15 cm/s^2 , with a RMS acceleration of 5 cm/s^2 (Australian/New Zealand Standard, 2002). It is a serviceability requirement. The design constraints specified for the benchmark problem are the RMS control force $\sigma_u \leq 100 \text{ kN}$, the RMS actuator stroke $\sigma_{x_m} \leq 30 \text{ cm}$, the maximum control force $\max|u(t)| \leq 300 \text{ kN}$ and the maximum stroke $\max|x_m(t)| \leq 95 \text{ cm}$.

3.2 Performance evaluation criteria

To systematically evaluate the control performance of comparative controllers, twelve performance criteria were introduced in the benchmark problem as shown in Table 1. From the response time histories, the peak response quantities can be obtained and the temporal RMS values are computed.

Table 1 Performance criteria of the benchmark problem

| Index | Description |
|----------|---|
| J_1 | maximum floor RMS acceleration |
| J_2 | average RMS acceleration for selected floors |
| J_3 | maximum RMS displacement of top floor |
| J_4 | average RMS displacement for selected floors |
| J_5 | RMS actuator stroke |
| J_6 | RMS control power |
| J_7 | maximum floor peak acceleration |
| J_8 | average peak acceleration for selected floors |
| J_9 | maximum peak displacement of top floor |
| J_{10} | average peak displacement for selected floors |
| J_{11} | peak actuator stroke |
| J_{12} | peak control power |

In the performance indices, the controlled responses are normalized by the corresponding responses in the uncontrolled benchmark building. Thus, smaller numbers represent a more effective response control performance. The first six performance measures (J_1 - J_6) are root-mean-square (RMS) responses of the selected floors of the structure and actuator. The next six performance measures (J_7 - J_{12}) are the peak responses of the selected floors of the structure and actuator. Information on the selected floors of each performance index is presented in the benchmark problem (Yang *et al.* 2004).

4. Development of hierarchical fuzzy hybrid controller

4.1 Skyhook and groundhook control strategies

For vehicle systems, it is known that skyhook strategy can enhance vehicle ride comfort by reducing vehicle body vibration and the groundhook damping control policy can enhance vehicle stability by suppressing wheel axle vibration. For civil structure applications, skyhook controller can effectively reduce the vibration of the auxiliary mass, i.e., the STMD. On the other hand, groundhook controller shows good control performance for the reduction of structure responses (Setareh 2001). The idealized configurations of both the skyhook and groundhook controllers are shown in Fig. 4. These ideal skyhook and groundhook configurations cannot be realized in practice because the damper cannot be fixed to the sky or a non-moving inertia frame. Therefore, the goal of skyhook or groundhook semi-active control policies is to emulate the ideal structural configuration of a passive damper “hooked” between the structure and the “sky” or the “ground”, respectively, by using the real configuration of the STMD shown in Fig. 1. Among various versions of groundhook control algorithms, the displacement-based on-off groundhook controller (Koo *et al.* 2004) is employed in this study. Although the system used by Koo *et al.* (2004) is very different from the building structure used here and is subjected to a different type of excitation, the displacement-based on-off groundhook control policy shows the best performance for the benchmark problem

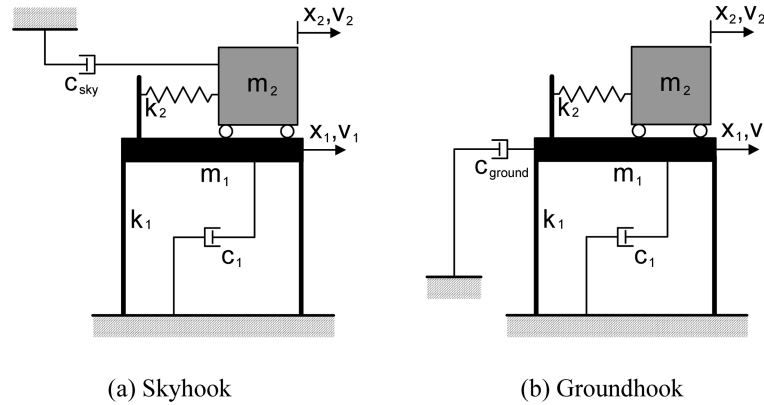


Fig. 4 Idealized semi-active control configurations

among four control policies investigated by Koo *et al.* (2004).

Referring to Fig. 4, the relative velocity is defined by subtracting the velocity of the STMD from that of the structure, i.e., $v_1 - v_2$. The displacement-based skyhook control policy is defined by using the relative velocity and the displacement of the STMD (x_2). In the case of the on-off skyhook control algorithm, the command voltage is switched between a minimum and a maximum level. The switching is performed based on the following conditions

$$V = \begin{cases} V_{\max} & \text{if } x_2(v_1 - v_2) \leq 0 \\ V_{\min} & \text{if } x_2(v_1 - v_2) > 0 \end{cases} \quad (1)$$

where, V is the command voltage, V_{\max} is the maximum voltage, namely 5 V, V_{\min} is the minimum voltage, 0 V.

The displacement-based on-off skyhook control policy can be evolved to the groundhook control policy by changing x_2 to x_1 . The groundhook control algorithm used in this study is given by

$$V = \begin{cases} V_{\max} & \text{if } x_1(v_1 - v_2) \geq 0 \\ V_{\min} & \text{if } x_1(v_1 - v_2) < 0 \end{cases} \quad (2)$$

As observed in Eqs. (1) and (2), the command voltage based on skyhook or groundhook control is determined by a very simple computation. Because of this simplicity, they have been favorably used for real-time control and successfully applied to vehicle vibration control and civil structure control with good performance.

A numerical simulation of the benchmark building has been performed to investigate the control effectiveness of skyhook and groundhook control policies for the STMD. The peak and RMS responses of the STMD and the structure are compared for selected floors as shown in Table 2. The response quantities of the uncontrolled case are also presented for comparison purpose. Results from numerical simulation demonstrate that the groundhook controller provides a significantly superior control performance over the skyhook controller for all the structure responses. When groundhook controller is used, the peak and RMS accelerations of the 75th floor are 13.36 cm/sec^2 and 3.91 cm/sec^2 , respectively. And they are less than the maximum allowable floor acceleration of 15 cm/sec^2

Table 2 Peak and RMS response quantities of sub-controllers and uncontrolled case

| Floor No. | Skyhook | | | | Groundhook | | | | No control | | | |
|-----------|--------------|-------------|--------------|-------------|---------------|--------------|--------------|-------------|------------|-------|-------|------|
| | Peak | | RMS | | Peak | | RMS | | Peak | | RMS | |
| | Disp. | Acc. | Disp. | Acc. | Disp. | Acc. | Disp. | Acc. | Disp. | Acc. | Disp. | Acc. |
| 1 | 0.04 | 0.21 | 0.01 | 0.06 | 0.04 | 0.22 | 0.01 | 0.06 | 0.05 | 0.22 | 0.02 | 0.06 |
| 30 | 5.47 | 4.15 | 1.4 | 1.14 | 4.93 | 3.74 | 1.24 | 0.95 | 6.84 | 7.14 | 2.15 | 2.02 |
| 50 | 13.04 | 8.26 | 3.37 | 2.54 | 11.69 | 7.18 | 2.99 | 2.02 | 16.59 | 14.96 | 5.22 | 4.78 |
| 55 | 15.18 | 9.21 | 3.94 | 2.95 | 13.6 | 8.23 | 3.49 | 2.34 | 19.41 | 17.48 | 6.11 | 5.59 |
| 60 | 17.38 | 10.76 | 4.53 | 3.36 | 15.56 | 9.37 | 4.01 | 2.66 | 22.34 | 19.95 | 7.02 | 6.42 |
| 65 | 19.63 | 12.33 | 5.13 | 3.84 | 17.56 | 10.26 | 4.54 | 3.05 | 25.35 | 22.58 | 7.97 | 7.31 |
| 70 | 21.9 | 13.99 | 5.75 | 4.33 | 19.58 | 11.67 | 5.08 | 3.42 | 28.41 | 26.04 | 8.92 | 8.18 |
| 75 | 24.25 | 16.6 | 6.38 | 4.85 | 21.67 | 13.36 | 5.64 | 3.91 | 31.59 | 30.33 | 9.92 | 9.14 |
| 76 | 24.77 | 17.34 | 6.52 | 4.98 | 22.14 | 14.53 | 5.77 | 3.98 | 32.30 | 31.17 | 10.14 | 9.35 |
| STMD | 66.89 | 72.4 | 16.99 | 18.03 | 106.32 | 109.06 | 30.74 | 30.55 | - | - | - | - |

and the RMS value of 5 cm/sec², respectively. However, the peak and RMS displacements of the STMD are 106.32 cm and 30.74 cm as shown in Table 2. They exceed the control constraints given by 95 cm and 30 cm, respectively. On the other hand, a skyhook controller can easily satisfy the control constraints of the STMD displacement by providing the peak value of 66.89 cm and the RMS value of 16.99 cm. However, the peak acceleration of the 75th floor is 16.60 cm/sec², and it is greater than the maximum allowable floor acceleration. Based on numerical simulation, it is found that neither of the two controllers can satisfy the design requirement of the benchmark building by oneself.

4.2 Combination of sub-controllers using a weighted sum approach

To satisfy the design requirement of the benchmark problem by using groundhook and skyhook controllers, a hybrid control technique is introduced in this study. There are several methods that can be used to combine multiple control signals to make a single control command. One of these methods, a weighted sum approach, is widely used because of its simplicity and intuitive understanding. Using the conventional weighted sum approach, a hybrid control strategy which combines two sub-controllers can be easily developed as follows

$$V = wV_{sky} + (1-w)V_{ground} \quad (3)$$

where V is the combined command voltage, V_{sky} is the command voltage generated by the skyhook controller, V_{ground} is the command voltage generated by the groundhook controller, and w is a weighting factor. In this hybrid control strategy, the participation of each controller can be conveniently adjusted by changing the weighting factor.

Eleven numerical simulation runs, where w varied from 0 to 1 in steps of 0.1, have been conducted to determine an appropriate weighting factor that can satisfy the design requirement of the benchmark problem. As observed in Eq. (3), if w is smaller than 0.5, the participation of the skyhook controller decreases in comparison with the groundhook controller. Among the control

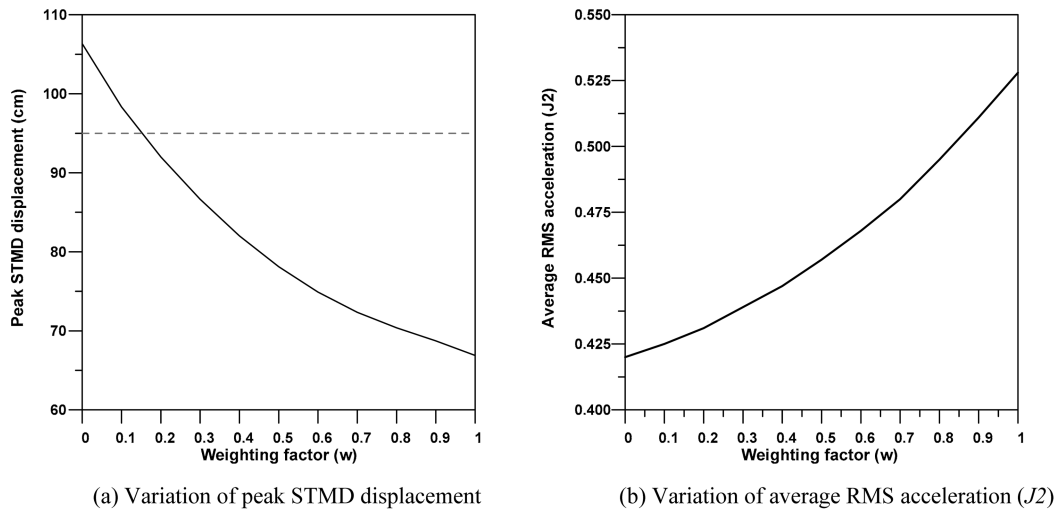


Fig. 5 Variation of responses according to weighting factor

constraints, the maximum stroke of a control device is one of critical conditions for real applications. The average RMS acceleration criterion (J_2) out of twelve performance criteria is one of the most important indices because it is directly associated with the occupant's discomfort. Therefore, the peak displacements of the STMD and J_2 are presented with variation of the weighting factor in Fig. 5. As the weighting factor increases, the participation of the skyhook controller increases, but the effect of the groundhook controller is reduced. In this case, the STMD displacement decreases and J_2 increases as can be seen in Fig. 5. In a conventional hybrid control technique using a weighted sum approach, an engineer needs to select an appropriate weighting factor that can satisfy the performance requirements. To this end, a number of numerical simulation runs with various weighting factors are necessary and this may involve considerable computation time and effort. In the conventional combination method using a weighted sum approach, the weighting factor is fixed after it is determined by an engineer. In this case, the participation of each sub-controller cannot be changed in real time, and thus adaptability of the conventional combination method may be poor. Recognizing these limitations, the fuzzy hybrid control technique has been developed in this study.

4.3 Fuzzy hybrid controller

In this study, a fuzzy hybrid control technique is developed to change the participation of each sub-controller in real time for more effective control of a wind-excited tall building using the STMD. In the proposed method, a fuzzy logic controller is used to change a weighting factor based on dynamic responses of the STMD and the structure as shown in Fig. 6. When the dynamic response of the structure increases, the fuzzy hybrid controller needs to decrease a weighting factor to increase the effect of the groundhook controller. On the other hand, a weighting factor should be decreased to augment the participation of the skyhook controller when the STMD motion is considerable.

Usually, Fuzzy logic maps an input space to an output space by means of if-then rules (Yen and

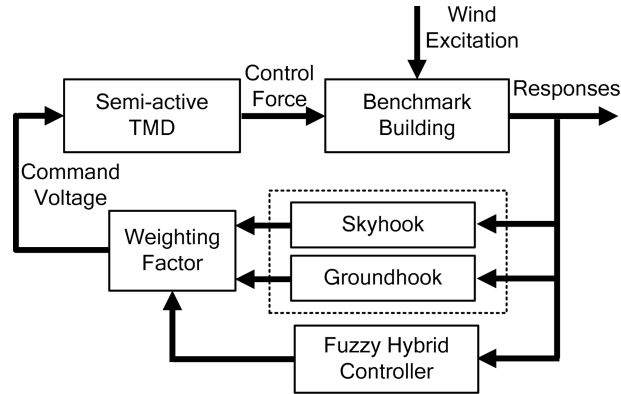


Fig. 6 Flow of fuzzy hybrid control using semi-active TMD



Fig. 7 Input and output relationships of fuzzy hybrid controller

Langari 1999). Control components of the input signal are transformed into linguistic values through a fuzzification interface at each time step. For output, the mapped linguistic values are transformed into numerical values through a defuzzification interface. The design of a fuzzy logic controller is separated into three parts: (1) define the number of input and output variables and choose the type of inference to be used; (2) define membership functions for the input and output variables; and (3) define if-then rules. In this study, the absolute values of the STMD displacement and the acceleration of the 75th floor are selected as inputs. The output is then the weighting factor as shown in Fig. 7. The fuzzy hybrid controller determines the weighting factor in real time based on two input variables. The number of membership functions used for two inputs are four, while six membership functions are used for the output. The input subsets are ‘huge’, ‘big’, ‘small’, and ‘zero’. The output variable is divided into six levels from w_0 to w_5 . Triangular membership functions are used for all input and output variables as shown in Figs. 8, 9 and 10.

Since each of output membership functions is fixed with an equally divided range as shown in Fig. 10, the performance of a fuzzy hybrid controller is mainly determined by the range of each membership function for two inputs. If once the range of the ‘huge’ membership function is determined, the other membership functions, i.e., ‘big’, ‘small’, and ‘zero’, can be directly defined by equally dividing a lower range than the ‘huge’ membership function as shown in Figs. 8 and 9. Therefore, the design of a fuzzy hybrid controller is mainly dependent on how to set the ‘huge’ membership function. If the ‘huge’ membership function for input 1 is set to be much lower than the maximum allowable displacement of the STMD (i.e., 95 cm), a fuzzy hybrid controller recognizes the relatively small displacement of the STMD as ‘huge’ input 1. Accordingly, a fuzzy hybrid controller tries to reduce the ‘huge’ STMD displacement, i.e., a fuzzy hybrid controller focuses on reduction of the STMD displacement. On the other hand, when the ‘huge’ membership

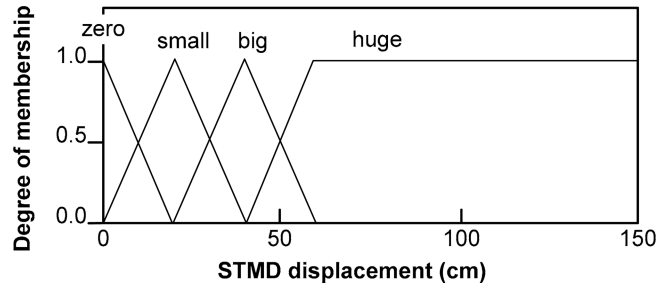


Fig. 8 Membership functions of input1: STMD displacement (cm)

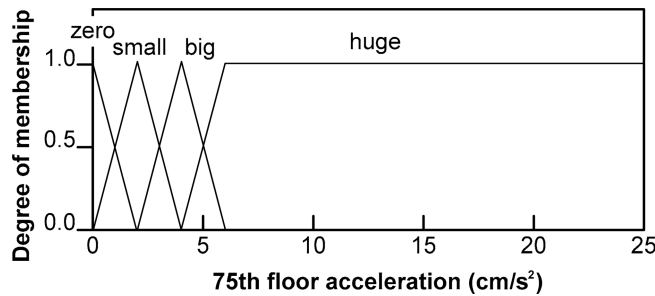


Fig. 9 Membership functions of input2: 75th floor acceleration (cm/s²)

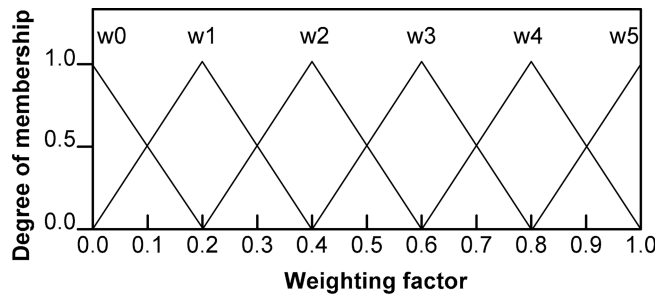


Fig. 10 Membership functions of output: weighting factor

function for input 2 is selected to be much lower than the maximum allowable acceleration of the building (i.e., 15 cm/s²), a fuzzy hybrid controller recognizes that input 2 is ‘huge’ with a relatively small acceleration of the building. Therefore, a fuzzy hybrid controller tries to decrease an output weighting factor to increase the effect of the groundhook controller that reduce the floor acceleration of the building with the increase of the STMD movement. Based on this characteristics of a fuzzy hybrid controller, numerical simulations have been conducted by varying the ranges of membership functions for input 1 and input 2. For example, if the building response is excessive, the starting value of the ‘huge’ membership function for input 2 is controlled to be decreased and that for input 1 is set to be a bigger value. When the STMD response exceeds the maximum limits, the starting value of the ‘huge’ membership function for input 1 needs to be decreased and that for input 2 is required to be increased. In this study, an iterative method for input membership functions

has been performed to select a suitable controller, which can appropriately reduce both building and STMD responses. Consequently, the ‘huge’ membership function for input 1 starts from 40 cm as shown in Fig. 8. Each triangular membership function of ‘big’, ‘small’, and ‘zero’ for input 1 is defined with the representative quantitative values of 40 cm, 20 cm, and 0 cm, respectively, and the range of them is set to be 40 cm. In the case of input 2, the ‘huge’ membership function starts from 4 cm/sec². The representative quantitative values of the other membership functions, i.e., ‘big’, ‘small’, and ‘zero’, are defined as 4 cm/sec², 2 cm/sec², and 0 cm/sec², respectively, with the range of 4 cm/sec². Accordingly, when the STMD displacement (input 1) exceeds 42% of the maximum allowable limit, the fuzzy hybrid controller assumes it is ‘huge’. On the other hand, the 75th floor acceleration (input 2) is judged to be ‘huge’ when it exceeds 27% of the maximum allowable limit. With a relatively small value of the 75th floor acceleration, the developed fuzzy hybrid controller recognizes that input 2 is ‘huge’. This means that the fuzzy hybrid controller focuses on the reduction of the 75th floor acceleration rather than the STMD displacement. It can be confirmed by the weighting factors generated by the developed fuzzy hybrid controller. This is presented in the following section.

Table 3 shows the corresponding fuzzy rules with two inputs and one output. In the table, the superscript denotes the rule number. The fundamental approach to design for the fuzzy hybrid controller is to minimize both the structure response and the STMD motion. To this end, the developed controller divides the responses of two inputs into four levels as shown in the Table. When the STMD response is very small (almost zero), reduction of the 75th floor acceleration is the primary purpose of the fuzzy hybrid controller. Thus, the weighting factor is specified to be ‘small’ (w0 or w1) to increase the effect of the groundhook controller. On the other hand, when the STMD motion is ‘huge’, the weighting factor needs to be ‘big’ (w4 or w5) to augment the contribution of the skyhook controller. When the STMD motion is moderate, the weighting factor is increased from w0 to w4 in inverse proportion to the 75th floor acceleration as observed in Table 3.

In this study, fuzzy logic controller maps a given input to an output weighting factor through five steps as follows. Step 1: Fuzzy inputs. Step 2: Apply fuzzy operator. Step 3: Apply implication method. Step 4: Aggregate all outputs. Step 5: Defuzzify (Yen and Langari 1999, Tanaka 2007). To describe this process more specifically, an example with specific inputs is used. Let’s assume that input 1 is 27 cm and input 2 is 7.8 cm/s². Based on Fig. 8, the value of input 1 (27 cm) is partially included in ‘small’ membership function and it is also considered to be ‘big’ input somewhat. This is a characteristics of fuzzy reasoning. The 75th floor acceleration of 7.8 cm/s² for input 2 is solely included in ‘huge’ membership function. Therefore, it can be seen that the rule 8 and rule 12 out of sixteen fuzzy rules in Table 3 are involved in this case. With the selected inputs, a fuzzy hybrid

Table 3 Rule base of fuzzy hybrid controller

| | | STMD displacement | | | |
|----------------------------|-------|--------------------|-------------------|--------------------|--------------------|
| | | Zero | Small | Big | Huge |
| 75th floor acceleration | Zero | w1 ^{(1)*} | w3 ⁽⁵⁾ | w4 ⁽⁹⁾ | w5 ⁽¹³⁾ |
| | Small | w1 ⁽²⁾ | w2 ⁽⁶⁾ | w3 ⁽¹⁰⁾ | w5 ⁽¹⁴⁾ |
| | Big | w0 ⁽³⁾ | w1 ⁽⁷⁾ | w2 ⁽¹¹⁾ | w4 ⁽¹⁵⁾ |
| | Huge | w0 ⁽⁴⁾ | w0 ⁽⁸⁾ | w1 ⁽¹²⁾ | w4 ⁽¹⁶⁾ |

*(1)-(12): Rule number

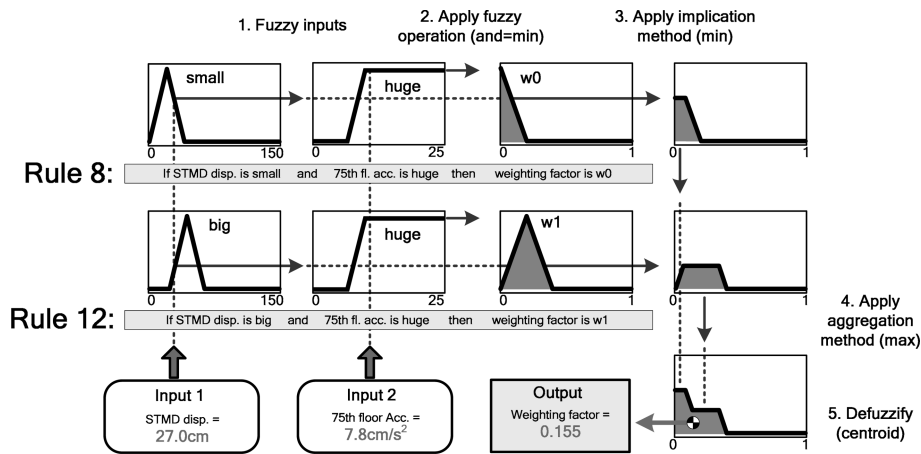


Fig. 11 Five steps of fuzzy hybrid controller

controller determines the output weighting factor through five steps as illustrated in Fig. 11. When the fuzzy inputs are entered, the fuzzy operator is applied to the two fuzzified inputs. In this study, the ‘minimum’ function is used for the ‘and’ fuzzy operator. After that, the output fuzzy sets are truncated using the ‘minimum’ function. The truncated output fuzzy sets for each rule are then aggregated into a single output fuzzy set by the ‘maximum’ function. Finally the resulting set is defuzzified to a single number. For defuzzification, the centroid calculation which is the most popular defuzzification method is used in this study. Consequently, the output weighting factor is 0.155 in this example. If input 1 is changed from 27 cm to 28 cm, the output weighting factor is calculated to be 0.162. Through this process, a fuzzy hybrid controller allows fine resolution in output weighting factor.

5. Performance evaluation

In this study, time history analyses of 900 seconds with a time step of 0.001 sec are performed in order to investigate the control performance of the proposed fuzzy hybrid control technique using the STMD. It is known that a small time lag exists between the control command and the MR damper force due to the inductance in the coil in the damper’s electromagnet and the time constant of the MR fluid (Yang *et al.* 2002). In this study, this time lag is modeled with a first-order filter given by $\dot{v}_c = -\eta(v_c - v)$ where v is the command voltage determined by the proposed fuzzy hybrid controller, v_c is the control input defined by the first-order filter that accounts for the dynamics of the MR damper, and η is the time constant associated with the first-order filter ($\eta = 50 \text{ s}^{-1}$). Accordingly, the MR damper force is determined by v_c to consider time lag of the MR damper. The time history of the weighting factor provided by the fuzzy hybrid controller is presented in Fig. 12. It can be seen that the weighting factor varies between ‘0’ and ‘1’ during real-time control. The average time history of the weighting factor is 0.33. This means that the fuzzy hybrid controller emphasizes the effect of the groundhook controller rather than the skyhook controller. The weighting factor generated by the fuzzy hybrid controller can be modified by changing the shape or range of membership functions or the if-then rules. As described in previous section, an appropriate

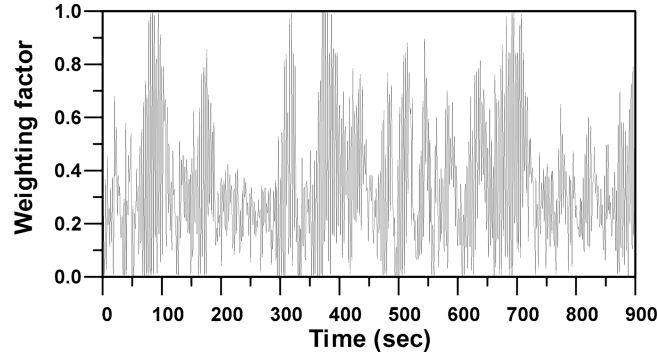


Fig. 12 Time history of weighting factor

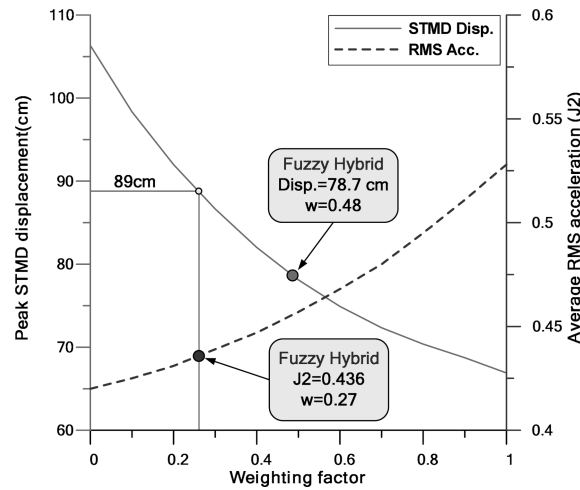


Fig. 13 Structural responses versus weighting factor

fuzzy hybrid controller is selected to satisfy the design requirements of the benchmark problem after the design and evaluation of several controllers.

In order to evaluate the performance of the fuzzy hybrid controller, the peak displacement of the STMD and J_2 provided by the fuzzy hybrid controller are presented in Fig. 13 along with those values obtained by the conventional hybrid control technique shown in Fig. 5. In the case of structural control of a wind-excited tall building using an STMD, a trade-off exists between responses of the STMD and the structure as observed in Fig. 13. Therefore, an improvement in one response cannot be achieved without detriment to another. When the fuzzy hybrid controller is used, the peak displacement of the STMD is 78.7 cm as shown in Fig. 13. The same STMD displacement occurs when the weighting factor of the conventional hybrid control technique is 0.48. The J_2 of the fuzzy hybrid controller is 0.436 and it is the same as that of the conventional hybrid control technique with the weighting factor of 0.27. However, when the conventional hybrid control technique is used, the peak displacement of the STMD is increased from 78.7 cm to 89 cm compared to the proposed fuzzy hybrid controller. From Fig. 13, it is found that the fuzzy hybrid controller can effectively reduce the structural responses without an increase of the STMD motion

Table 4 Comparison of performance criteria

| Index | STMD | | | TMD | ATMD |
|----------|------------|---------|--------------|-------|--------|
| | Groundhook | Skyhook | Fuzzy hybrid | | |
| J_1 | 0.428 | 0.531 | 0.444 | 0.589 | 0.369 |
| J_2 | 0.420 | 0.528 | 0.436 | 0.583 | 0.417 |
| J_3 | 0.569 | 0.643 | 0.581 | 0.681 | 0.578 |
| J_4 | 0.571 | 0.645 | 0.583 | 0.682 | 0.580 |
| J_5 | 3.032 | 1.676 | 2.564 | 1.258 | 2.271 |
| J_6 | 3.237 | 1.808 | 2.760 | 1.358 | 11.988 |
| J_7 | 0.441 | 0.547 | 0.441 | 0.652 | 0.381 |
| J_8 | 0.461 | 0.541 | 0.465 | 0.637 | 0.432 |
| J_9 | 0.685 | 0.767 | 0.677 | 0.786 | 0.717 |
| J_{10} | 0.694 | 0.775 | 0.685 | 0.794 | 0.725 |
| J_{11} | 3.292 | 2.071 | 2.435 | 1.319 | 2.299 |
| J_{12} | 3.494 | 2.167 | 2.540 | 1.384 | 71.869 |

compared to the conventional hybrid control technique.

Performance evaluation criteria of the groundhook, skyhook and fuzzy hybrid controller for the wind-excited benchmark building with the STMD are compared to those of the sample TMD and ATMD in Table 4. A comparison between groundhook and skyhook controllers shows that groundhook controller provides much better control performance for all the structure responses than skyhook controller. On the other hand, as expected, the performance criteria associated with the STMD response (J_5 and J_{11}) of the groundhook controller are worse than those of the skyhook controller. The control power criteria (J_6 and J_{12}) of the groundhook controller is also larger than that of the skyhook controller. The control performance of the fuzzy hybrid controller is comparable to that of the groundhook controller, but with a reduction in the STMD response. Table 4 shows that the control performance of the STMD controlled by the fuzzy hybrid controller is superior to that of the sample TMD. In comparison with the ATMD, the STMD provides a good performance for reduction in displacement response. This may be because the displacement-based control algorithms are employed as sub-controllers to control the STMD. In particular, the performance criteria associated with the peak displacement response (J_9 and J_{10}) of the STMD is better than those of the ATMD. It should be noted that the average and peak control power (J_6 and J_{12}) of the STMD are significantly smaller than those of the ATMD, while providing a similar control performance.

The peak and RMS response quantities for the selected floors (levels 1, 30, 50, 55, 60, 65, 70, 75, and 76) are summarized in Table 5. For the sample TMD, the peak and RMS acceleration response quantities on the 75th floor (19.79 cm/sec^2 and 5.38 cm/sec^2) are larger than the allowable peak and RMS floor acceleration, i.e., 15 cm/sec^2 and 5 cm/sec^2 . Thus, the sample TMD does not satisfy the design requirement of the benchmark building. When the ATMD is used, the response of the mass damper increases compared to the TMD. However, it satisfies the design requirement when excluding the 76th floor, which has no occupants. In the case of the STMD, all the structural responses are significantly reduced compared to the passive TMD. Moreover, the peak displacement response quantities of all the floors are less than those of the ATMD. The peak and RMS stroke of

Table 5 Comparison of structural response quantities

| Floor No. | STMD (Fuzzy hybrid) | | | | TMD | | | | ATMD | | | |
|-------------|---------------------|-------|-------|-------|-------|-------|-------|-------|-------|-------|-------|------|
| | Peak | | RMS | | Peak | | RMS | | Peak | | RMS | |
| | Disp. | Acc. | Disp. | Acc. | Disp. | Acc. | Disp. | Acc. | Disp. | Acc. | Disp. | Acc. |
| 1 | 0.04 | 0.21 | 0.01 | 0.06 | 0.04 | 0.21 | 0.01 | 0.06 | 0.04 | 0.23 | 0.01 | 0.06 |
| 30 | 4.87 | 3.81 | 1.27 | 0.97 | 5.60 | 4.68 | 1.48 | 1.23 | 5.14 | 3.37 | 1.26 | 0.89 |
| 50 | 11.55 | 7.25 | 3.05 | 2.10 | 13.34 | 9.28 | 3.57 | 2.79 | 12.22 | 6.73 | 3.04 | 2.03 |
| 55 | 13.44 | 8.36 | 3.57 | 2.44 | 15.54 | 10.74 | 4.17 | 3.26 | 14.22 | 8.05 | 3.55 | 2.41 |
| 60 | 15.37 | 9.53 | 4.10 | 2.77 | 17.80 | 12.70 | 4.79 | 3.72 | 16.27 | 8.93 | 4.08 | 2.81 |
| 65 | 17.35 | 10.39 | 4.64 | 3.18 | 20.10 | 14.72 | 5.43 | 4.25 | 18.36 | 10.05 | 4.62 | 3.16 |
| 70 | 19.34 | 11.63 | 5.19 | 3.57 | 22.43 | 16.77 | 6.08 | 4.76 | 20.48 | 10.67 | 5.17 | 3.38 |
| 75 | 21.40 | 13.37 | 5.77 | 4.06 | 24.84 | 19.79 | 6.75 | 5.38 | 22.67 | 11.56 | 5.74 | 3.34 |
| 76 | 21.87 | 14.56 | 5.89 | 4.14 | 25.38 | 20.52 | 6.90 | 5.48 | 23.15 | 15.89 | 5.86 | 4.70 |
| Mass Damper | 78.65 | 83.12 | 25.99 | 26.43 | 42.6 | 46.18 | 12.76 | 13.86 | 74.27 | 72.64 | 23.03 | 22.4 |

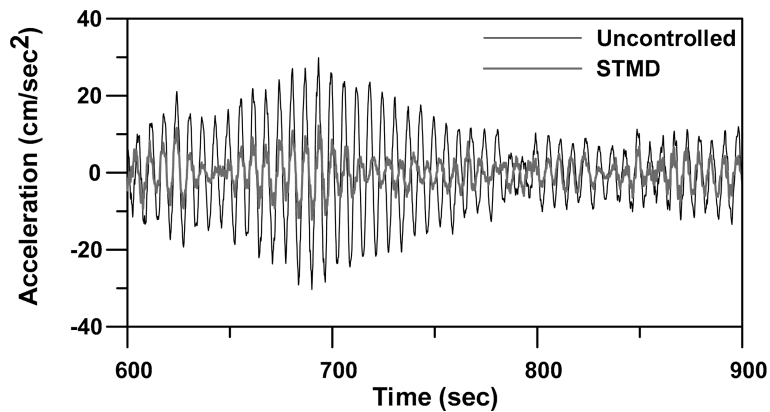


Fig. 14 Acceleration time history of the 75th floor

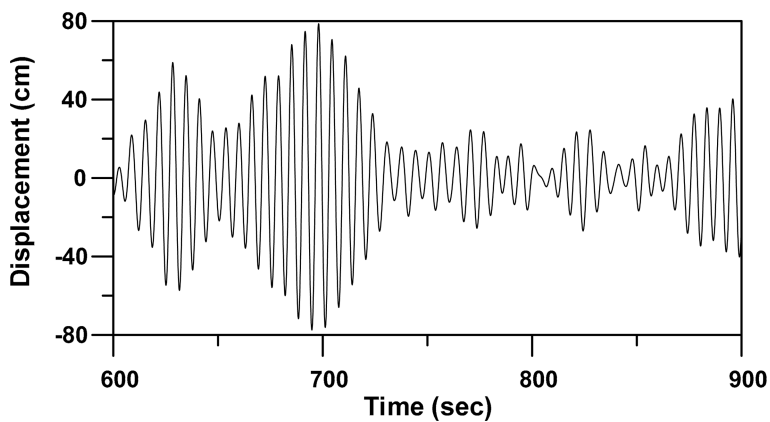


Fig. 15 STMD stroke time history

Table 6 Robustness of TMD and STMD

| | | RMS responses | | | | Peak responses | | | |
|-------|------------------|---------------|------------------|-------|----------|------------------|-------|------------------|-------|
| Index | $\Delta K=-15\%$ | | $\Delta K=+15\%$ | | Index | $\Delta K=-15\%$ | | $\Delta K=+15\%$ | |
| | TMD | STMD | TMD | STMD | | TMD | STMD | TMD | STMD |
| J_1 | 0.594 | 0.538 | 0.494 | 0.455 | J_7 | 0.695 | 0.619 | 0.556 | 0.523 |
| J_2 | 0.586 | 0.53 | 0.488 | 0.449 | J_8 | 0.697 | 0.613 | 0.557 | 0.497 |
| J_3 | 0.809 | 0.768 | 0.526 | 0.501 | J_9 | 0.999 | 0.897 | 0.633 | 0.637 |
| J_4 | 0.81 | 0.769 | 0.527 | 0.503 | J_{10} | 1.008 | 0.904 | 0.637 | 0.643 |

the STMD are 78.65 cm and 25.99 cm, respectively, which are less than the prescribed limit. Numerical results show that the STMD satisfies the design requirement including the 76th floor.

The acceleration time histories of the 75th floor of the STMD-controlled and the uncontrolled cases are shown in Fig. 14. The STMD stroke time history is also presented in Fig. 15. In order to clarify the difference between the STMD-controlled response and the uncontrolled response, the response time histories are presented only for a duration of 300 sec as shown in Figs. 14 and 15. The acceleration response of the STMD-controlled case is significantly less than that of the uncontrolled case as observed in Fig. 14. Specifically, the difference between the responses of the STMD-controlled and the uncontrolled cases is significant around 700 sec, where the responses of the benchmark building are most excessive. Accordingly, the STMD appears to be very effective for controlling excessive vibrations that can cause damage to the structure. As can be seen in Fig. 15, a bigger movement of the STMD is required to reduce the excessive response of the building. And it can be recognized that the peak STMD stroke is less than the maximum allowable STMD stroke (i.e., 95 cm).

In addition to the control performance, the robustness is one of the most important features of control devices. The benchmark problem suggested that the robustness of the proposed controller should be discussed because the variation of the structure's frequency may cause significant performance deterioration. To investigate the robustness of the proposed STMD, the performance criteria of the sample TMD and STMD are compared for stiffness uncertainties of $\pm 15\%$ as shown in Table 6. Among the twelve criteria, only eight criteria (J_1 - J_4 and J_7 - J_{10}) are used because the other criteria represent the performance of the mass damper. Numerical results show that the robustness of the STMD is better than that of the passive TMD, although the control effects of the STMD are deteriorated with stiffness variation. In the case of the passive TMD, the J_{10} is larger than '1'; thus it may amplify the structural responses of the benchmark building under a stiffness uncertainty of -15% .

6. Conclusions

This study investigates the control performance of a fuzzy hybrid controller for a wind-excited 76-story benchmark building using STMD. Since skyhook and groundhook control algorithms can effectively reduce dynamic responses of the STMD and the building structure, respectively, they are used as sub-controllers. In the proposed approach, the fuzzy hybrid controller modulates in real time two command voltages generated by sub-controllers into the appropriately combined command

voltage based on a simple fuzzy inference mechanism. The sample passive TMD and ATMD controlled by a LQG controller proposed in the benchmark problem are used as references for comparative studies. In addition, the STMD controlled by a conventional hybrid control technique is used to investigate the effectiveness of the proposed fuzzy hybrid control algorithm.

Results from numerical simulation demonstrate that neither the skyhook nor the groundhook controllers can satisfy the design requirement of the benchmark building on their own, and thus the hybrid control technique is required. The proposed fuzzy hybrid controller can effectively reduce both responses of the STMD and structure compared to the conventional hybrid control and it satisfies the design requirement of the benchmark building. The STMD controlled by the proposed fuzzy hybrid controller shows much better control performance than the sample TMD. Generally, numerical results of the STMD are comparable to those of the ATMD, whereas the control power of the STMD is substantially lower than that of the ATMD. For the reduction of the acceleration responses, the ATMD shows a better control performance than the STMD. However, the STMD can effectively reduce the displacement responses. For changes in stiffness of the structure, the STMD controlled by the proposed controller is less sensitive than the sample TMD. Consequently, the design requirements of the benchmark problem have been successfully achieved by the proposed controller satisfying the control device capacity constraints. However, even if an STMD shows better control performance than the passive TMD, an engineer should carefully consider introduction of an STMD by weighing the performance improvement against the additional cost associated with managing semi-active control system. Since the STMD with an MR damper having a reasonable capacity (100 kN) is successfully used to control the full-scale 76-story building, the STMD is expected to be a practical means for mitigating the wind-induced responses of a tall building.

Acknowledgements

This research was supported by a grant (code#06 R&D B03) from Cutting-edge Urban Development Program funded by the Ministry of Land, Transport and Maritime Affairs of Korean government.

References

- Ankireddi, S. and Yang, H.T.Y. (1996), "Simple ATMD control methodology for tall buildings subject to wind loads", *J. Struct. Eng.*, **122**, 83-91.
- Australian/New Zealand Standard (2002), *Structural Design Actions: Wind Actions*, AS1170-2:2002, Standards Australia, Sydney.
- Chang, J.C.H. and Soong, T.T. (1980), "Structural control using active tuned mass damper", *J. Eng. Mech.*, **106**, 1091-1098.
- Den Hartog, J.P. (1956), *Mechanical Vibrations*, 4th Edition, McGraw-Hill, New York.
- Hidaka, S., Ahn, Y.K. and Morishita, S. (1999), "Adaptive vibration control by a variable-damping dynamic absorber using ER fluid", *J. Vib. Acoust.*, **121**, 373-378.
- Hrovat, D., Barak, P. and Rabins, M. (1983), "Semi-active versus passive or active tuned mass damper for structural control", *J. Eng. Mech.-ASCE*, **190**(3), 691-705.
- Jansen, L.M. and Dyke, S.J. (1999), "Semiactive control strategies for MR dampers: comparative study", *J. Eng. Mech.*, **126**(8), 796-803.

- Karnopp, D., Crosby, M.J. and Harwood, R.A. (1974), "Vibration control using semi-active force generators", *J. Eng. Ind., ASME*, **96**(2), 619-626.
- Koo, J.H., Ahmadian, M. and Setareh, M. (2006), "Experimental robustness analysis of magneto-rheological tuned vibration absorbers subject to mass off-tuning", *J. Vib. Acoust.*, **128**(1), 126-131.
- Koo, J.H., Setareh, M. and Murray, T.M. (2004), "In search of suitable control methods for semi-active tuned vibration absorbers", *J. Vib. Acoust.*, **10**, 163-174.
- Liu, Y., Waters, T.P. and Brennan, M.J. (2005), "A comparison of semi-active damping control strategies for vibration isolation of harmonic disturbances", *J. Sound Vib.*, **280**, 21-39
- Nagarajaiah, S. and Varadarajan, N. (2000), "Novel semiactive variable stiffness tuned mass damper with real time tuning capability", *Proceedings of the 13th Engineering Mechanics Conference*, Reston.
- Narasimhan, S. and Nagarajaiah, S. (2006), "Phase I smart base isolated benchmark building sample controllers for linear isolation system: Part II", *Struct. Control Hlth.*, **13**, 589-604.
- Narasimhan, S., Nagarajaiah, S., Johnson, E.A. and Gavin, H.P. (2006), "Smart base isolated benchmark building Part I: problem definition", *Struct. Control Hlth.*, **13**, 573-588.
- Ohtori, Y., Christenson, R.E., Spencer, B.F., Jr. and Dyke, S.J. (2004), "Benchmark control problems for seismically excited nonlinear buildings", *J. Eng. Mech.*, **130**(4), 366-385.
- Pinkaew, T. and Fujino, Y. (2001), "Effectiveness of semi-active tuned mass dampers under harmonic excitation", *Eng. Struct.*, **23**, 850-856.
- Ricciardella, F., Occhiuzzib, A. and Clemente, P. (2000), "Semi-active tuned mass damper control strategy for wind-excited structures", *J. Wind Eng. Ind. Aerod.*, **88**, 57-74.
- Samali, B., Kwok, K.C.S., Wood, G.S. and Yang, J.N. (2004), "Wind tunnel tests for wind-excited benchmark building", *J. Eng. Mech.-ASCE*, **130**(4), 437-446.
- Setareh, M. (2001), "Use of semi-active tuned mass dampers for vibration control of force-excited structures", *Struct. Eng. Mech.*, **11**(4), 341-356.
- Sues, R.H., Mau, S.T. and Wen, Y.K. (1988), "System identification of degrading hysteretic restoring forces", *J. Eng. Mech.-ASCE*, **114**(5), 833-846.
- Tanaka, K. (2007), *An Introduction to Fuzzy Logic for Practical Applications*, Rassel, Inc.
- Warburton, G.B. and Ayorinde, E.O. (1980), "Optimum absorber parameters for simple systems", *Earthq. Eng. Struct. Dyn.*, **8**, 197-217.
- Yang, G., Spencer, Jr., B.F., Carlson, J.D. and Sain, M.K. (2002), "Large-scale MR fluid dampers: modeling and dynamic performance considerations", *Eng. Struct.*, **24**, 309-323.
- Yang, J.N., Agrawal, A.K., Samali, B. and Wu, J.C. (2004), "Benchmark problem for response control of wind-excited tall buildings", *J. Eng. Mech.-ASCE*, **130**(4), 437-446.
- Yen, J. and Langari, R. (1999), *Fuzzy Logic: Intelligence, Control, and Information*, Prentice Hall, Inc., New York.